CLEC10A expression defines functionally distinct subsets of conventional type 2 dendritic cells (cDC2) in the mouse lung

CLEC10A expression defines functionally distinct subsets of conventional type 2 dendritic cells (cDC2) in the mouse lung

Fumiya Nihashi [a], Kazuki Furuhashi [a,b,c*], Ryo Horiguchi [d], Yoshihiro Kitahara [a], Yusuke Inoue [a], Hideki Yasui [a], Masato Karayama [a], Yuzo Suzuki [a], Hironao Hozumi [a], Noriyuki Enomoto [a], Tomoyuki Fujisawa [a], Yutaro Nakamura [a], Naoki Inui [a], Takafumi Suda [a]

[a] Second Division, Department of Internal Medicine, Hamamatsu University School of Medicine

[b] Department of Laboratory Medicine, Hamamatsu University School of Medicine

[c] Infection Control and Prevention Center, Hamamatsu University School of Medicine

[d] Advanced Research Facilities and Services, Hamamatsu University School of Medicine

***Corresponding author:** Kazuki Furuhashi, 1-20-1 Handayama, Hamamatsu 431-3192, Japan; Tel: +81(53) 435-2799; Fax: +81(53) 435-2456; E-mail: k.furu@hama-med.ac.jp

Conflict of interest statement

The authors declare no conflict of interest.

Authors' contributions

FN and KF designed the study, performed the experiments, and collected the data. RH and FN contributed to the laboratory work. All authors performed data analysis and interpretation of the results. FN, KF and TS wrote the manuscript. All authors read and approved the final manuscript.

30 ***Dear Editor,***

31

32 Lung dendritic cells (LDCs) are crucial for the immune response in diseases like
33 asthma and allergic airway disorders. Dendritic cells are categorized mainly into
34 conventional DCs (cDCs) with antigen-presenting abilities and plasmacytoid DCs that
35 produce type 1 interferons [1, 2]. cDCs can be classified into conventional type 1
36 (cDC1) and type 2 (cDC2). cDC2 plays a crucial role in activating $CD4^+$ T cells
37 primarily, while cDC1 stimulates preferentially $CD8^+$ T cells [2]. Recent studies
38 highlighted the heterogeneity within the cDC2, identifying two distinct cDC2 subsets in
39 the spleen based on C-type lectin domain family 10 member A (CLEC10A) and
40 CLEC12A [3, 4]. These two cDC2 subsets have been shown to be functionally distinct
41 in different organs, however, their roles in the mouse lung have not been fully
42 elucidated. CLEC10A is a C-type lectin receptor (CLR) belonging to a subfamily of
43 pattern recognition receptors dedicated to sensing glycans. CLRs expressed on
44 macrophages and DCs in multiple organs trigger cytokine production as well as
45 maintain homeostasis and immunomodulation. Additionally, the CLRs play an
46 important role in immune cell recruitment, T-cell differentiation, and antibody
47 production [4, 5, 6]. Interestingly, a recent study revealed that two splenic cDC2 subsets
48 based on CLEC10A expression differ in their expression levels of costimulatory
49 molecules and T-cell proliferative capacity [4]. Several CLRs activate DCs to
50 exacerbate allergic airway inflammation and induce $CD4^+$ T-cell responses, however,
51 little information is available on the newly identified cDC2 subset that expresses
52 CLEC10A in the lungs. In this study, we examined functional differences between two

53 cDC2 subsets classified by CLEC10A expression in a mouse model of ovalbumin
54 (OVA) stimulated asthma (Supplementary Methods).
55 Conventional LDC subsets were isolated as previously described [7] and classified
56 by flow cytometry (FACS) based on XCR1 and CD172a expression. cDC2 could be
57 further subdivided into CLEC10A^{+} and CLEC10A^{-} cDC2 based on their CLEC10A
58 expression (Fig. 1A). We generated sensitized mice with OVA (Fig. 1B) and identified
59 cDC subsets in the spleen, mediastinal lymph nodes (MLN), and lungs. CLEC10A^{+} and
60 CLEC10A^{-} cDC2 increased in proportion in the MLN and lungs more than in the spleen
61 after OVA sensitization (Fig. 1C), with significant increases in cell counts in the two
62 cDC2 subsets compared to cDC1 (Fig. 1D). To understand the genetic makeup of two
63 cDC2 subsets, RNA sequencing was conducted on purified CLEC10A^{+} and CLEC10A^{-}
64 cDC2 from OVA-primed lungs. This analysis identified 6,330 differentially expressed
65 genes between two cDC2 subsets (Fig. 1E). As shown in the volcano plot, the most
66 notably upregulated genes in CLEC10A^{+} cDC2 cells included *Cd209c*, whereas *Ace*
67 was downregulated. Gene set enrichment analysis (GSEA) [8] revealed that pathways
68 related to endopeptidase activator activity, MHC protein complex, and exogenous
69 protein binding were enriched in CLEC10A^{+} cDC2. In contrast, pathways involved in
70 binding to oligopeptide, peptidoglycan, proteoglycan, and protein activation cascade
71 were enriched in CLEC10A^{-} cDC2 (Fig. 1F). Additionally, CLEC10A^{+} cDC2 had
72 higher expression of transcription factors related to cDC2 differentiation (*Sirpa*, *Irf4*,
73 and *Klf4*) and costimulatory molecules (*Cd40*, *Cd80*, *Cd86,* and *Icosl*), whereas
74 CLEC10A^{-} cDC2 had elevated levels of RNA associated with particular cytokines and
75 receptors (*Il6*, *Il10*, *Il23a*, *Il27*, and *Il17ra*) (Fig. 1G). Regarding pattern recognition
76 receptors, RNA expression levels of various CLRs except for *Clec7a* and *Clec9a* were

77 higher in CLEC10A$^+$ cDC2 than in CLEC10A$^-$ cDC2, and RNA expression levels of
78 each Toll-like receptor also differed between the two cDC2 subsets.
79 When examining surface markers after OVA priming, both cDC2 subsets exhibited
80 high levels of MHC class II, CLEC12A, CD40, and CD80, but their mean fluorescence
81 intensity levels were significantly higher in CLEC10A$^+$ cDC2 than in CLEC10A$^-$ cDC2
82 (Fig. 2A). We evaluated the ability of OVA antigen phagocytosis using FACS.
83 CLEC10A$^+$ cDC2 had a much higher uptake rate of labeled OVA than CLEC10A$^-$
84 cDC2 (Fig. 2B-C). When co-cultured with OVA-specific naïve CD4$^+$ T cells from OT-
85 II mice, CLEC10A$^+$ cDC2 from the lungs induced significantly greater proliferation
86 rates of those T cells (Fig. 2D) and higher GATA3 expression compared to CLEC10A$^-$
87 cDC2 (Fig. 2E). Furthermore, IL-2 and IL-6 were significantly elevated in the
88 supernatant of CLEC10A$^+$ cDC2 co-cultures (Fig. 2F). IL-4 levels tended to be higher
89 in co-cultures of CLEC10A$^+$ cDC2 than those of CLEC10A$^-$ cDC2, but the difference
90 was not statistically significant. However, with respect to cytokine production capacity,
91 CLEC10A$^-$ cDC2 secreted significantly more IL-6 and TNF to various TLR ligands
92 than CLEC10A$^+$ cDC2, while there were no significant differences in IL-12p70 and
93 IFN-γ levels and no IL-10 was detected (Figure 2G).
94 Several studies have focused on CLEC10A expression to define cDC2 subsets in the
95 thymus, spleen, lymph nodes, skin, liver, and lungs of naïve mice [3, 4, 6, 9]. cDC2
96 expressing Mgl2, one of the homologs of CLEC10A facilitates CD4$^+$ T-cell
97 accumulation in superficial lymph nodes and is required to generate a Th2 response
98 after subcutaneous OVA administration [3]. More recently, sequencing of cDC2 in the
99 lungs revealed that after house-dust mite and OVA exposure, single-cell RNA
100 developed into five distinct clusters, including CLEC10A$^+$ cDC2 [9]. However, the

101 detailed functional roles of CLEC10A^{+} cDC2 in antigen phagocytosis, T-cell
102 proliferation, and cytokine production have not yet been fully elucidated. This study
103 showed that the CLEC10A^{+} cDC2 more effectively phagocyted antigen than
104 CLEC10A^{-} cDC2, and triggered antigen-specific CD4^{+} T-cell proliferation in OVA-
105 sensitized mice. Conversely, CLEC10A^{-} cDC2 was more adept at producing pro-
106 inflammatory cytokines. These results suggest that there are functionally distinct
107 subtypes of cDC2 in the mouse lung, defined by CLEC10A expression. Brown et al.
108 used cluster analysis based on single-cell survey to identify cDC2 subsets based on the
109 expression of T-bet in mouse spleen [4]. They showed that the CLEC10A^{+} cDC2, most
110 of which is double-positive for CLEC12A, is pro-inflammatory with high IL-6 and
111 TNF-α production, whereas the CLEC10A^{-} cDC2 is anti-inflammatory. Consistent with
112 their finding, most CLEC10A^{+} cDC2 cells in the mouse lung expressed CLEC12A.
113 However, in the lung, these CLEC10A^{+} cDC2 showed lower IL-6 and TNF productions
114 than CLEC10A^{-} cDC2, contradicting Brown's results. To explain conflicting results, we
115 examined T-bet expression levels between two cDC2 subsets classified by CLEC10A in
116 the mouse lungs using FACS and RNA-seq data (Supplementary table) and found no
117 difference (Data not shown). Since the cDC2 subsets they classified are targeted
118 differently from the cDC2 subsets we classified based on CLEC10A, we believe that
119 such differences are partially responsible for the difference between our results and
120 Brown's. Furthermore, these differences might arise from DCs located in diverse organs
121 or varied antigen stimulations. Nevertheless, these data suggest that CLEC10A
122 expression defines two functionally distinct cDC2 subsets in the mouse lung and that
123 CLEC10A^{+} cDC2 can induce T-cell immunity more efficiently.
124

Acknowledgments

This work was supported by a Grant-in-Aid for Scientific Research 19K17671 (KF) from the Japan Society for the Promotion of Science, Novartis Research Grants 2019 (KF), and Hamamatsu University School of Medicine (HUSM) Grant-in-Aid 42351E (FN). We thank Dr. Shigeo Koyasu and Dr. William R. Heath for the use of C57BL/6-Tg (TCR-OT-II.2) Cbn mice. We would like to thank Editage (www.editage.jp) for English language editing.

135 **References**

136 1. Guilliams M, Ginhoux F, Jakubzick C, Naik SH, Onai N, Schraml BU, et al.
137 Dendritic cells, monocytes and macrophages: a unified nomenclature based on
138 ontogeny. *Nat Rev Immunol* 2014; **14**: 571-8.
139 2. Nutt SL, Chopin M. Transcriptional networks driving dendritic cell differentiation
140 and function. *Immunity* 2020; **52**: 942-56.
141 3. Kumamoto Y, Linehan M, Weinstein JS, Laidlaw BJ, Craft JE, Iwasaki A.
142 CD301b^{+} dermal dendritic cells drive T helper 2 cell-mediated immunity. *Immunity*
143 2013; **39**: 733-43.
144 4. Brown CC, Gudjonson H, Pritykin Y, Deep D, Lavallée VP, Mendoza A, et al.
145 Transcriptional basis of mouse and human dendritic cell heterogeneity. *Cell* 2019;
146 **179**: 846-863.e24.
147 5. Brown GD, Willment JA, Whitehead L. C-type lectins in immunity and
148 homeostasis. *Nat Rev Immunol* 2018; **18**: 374-89.
149 6. Denda-Nagai K, Aida S, Saba K, Suzuki K, Moriyama S, Oo-Puthinan S, et al.
150 Distribution and function of macrophage galactose-type C-type lectin 2
151 (MGL2/CD301b): efficient uptake and presentation of glycosylated antigens by
152 dendritic cells. *J Biol Chem* 2010; **285**: 19193-204.
153 7. Sakurai S, Furuhashi K, Horiguchi R, Nihashi F, Yasui H, Karayama M, et al.
154 Conventional type 2 lung dendritic cells are potent inducers of follicular helper T
155 cells in the asthmatic lung. *Allergol Int* 2021; **70**: 351-9.
156 8. Subramanian A, Tamayo P, Mootha VK, Mukherjee S, Ebert BL, Gillette MA, et
157 al. Gene set enrichment analysis: a knowledge-based approach for interpreting
158 genome-wide expression profiles**.** *Proc Natl Acad Sci U S A*. 2005; **102**: 15545-50.

159 9. Izumi G, Nakano H, Nakano K, Whitehead GS, Grimm SA, Fessler MB, et al.
160 CD11b^{+} lung dendritic cells at different stages of maturation induce Th17 or Th2
161 differentiation. *Nat Commun* 2021; **12**: 5029.

162

163

164

165 **Figure legends**

166 **Fig. 1.** Identification and quantification of conventional lung dendritic cell (LDC)
167 subsets (conventional type1 lung dendritic cell (cDC1), CLEC10A$^+$ conventional type 2
168 lung dendritic cell (cDC2) and CLEC10A$^-$ cDC2) following ovalbumin (OVA) priming
169 and sensitization, coupled with an RNA sequencing examination of gene expression
170 differences between CLEC10A$^+$ cDC2 and CLEC10A$^-$ cDC2. **(A)** Cells in the gated
171 area were analyzed for CD45, lineage, MHC class II, CD11c, XCR1, and CD172a. **(B)**
172 Schematic protocol of ovalbumin (OVA) priming and sensitization. **(C)** The pie charts
173 show the proportion of three conventional DC subsets in the spleen, mediastinal lymph
174 node, and lung after OVA priming and sensitization, and **(D)** the line graph shows the
175 changes in the cell counts of three conventional LDC subsets per mouse lung. The blue
176 represents cDC1, the orange represents CLEC10A$^+$ cDC2, and the gray represents
177 CLEC10A$^-$ cDC2. Data are presented as the mean ± SEM (five mice/group). **(E)** Bar
178 graphs comparing the differentially expressed genes in CLEC10A$^-$ cDC2 compared
179 with CLEC10A$^+$ cDC2. The blue bar shows more genes with reduced levels of
180 expression in CLEC10A$^-$ cDC2 than in CLEC10A$^+$ cDC2, and the red bar shows genes
181 with increased levels of expression. p-value < 0.05 is used as the cut-off value for gene
182 expression in the CLEC10A$^+$ and CLEC10A$^-$ cDC2 groups. Volcano plot showing the
183 distribution of differentially expressed genes between CLEC10A$^+$ cDC2 and
184 CLEC10A$^-$ cDC2. The blue dots show more genes with reduced expression in
185 CLEC10A$^+$ cDC2 compared with CLEC10A$^-$ cDC2, and the red dots show increased
186 gene expression in CLEC10A$^+$ cDC2 compared with CLEC10A$^-$ cDC2. **(F)** Enrichment
187 of Gene Ontology pathways in CLEC10A$^+$ and CLEC10A$^-$ cDC2. The red bar shows
188 Molecular function set group, the green bar shows Cellular component set group, and

189 the blue bar shows Biological process set group. **(G)** Heatmap of RNA sequencing data
190 showing expression of genes associated with dendritic cell surface markers, cytokines,
191 C-type lectin receptors, and Toll-like receptors. The levels of expression are indicated
192 by color difference as shown in the top bar (four mice/group).
193
194 **Fig. 2.** Differences in characteristics and function between each CLEC10A conventional
195 type2 lung dendritic cell (cDC2) subset. **(A)** The levels of expression of costimulatory
196 molecules on CLEC10A^{+} cDC2 (top) and CLEC10A^{-} cDC2 (bottom) were analyzed by
197 FACS using the monoclonal antibodies indicated. Histograms show the expression
198 levels of the cell surface markers on stimulated cDC2 subsets (solid line, white area)
199 and unstimulated (shaded area). These results are representative of more than four
200 independent experiments. Mean fluorescence intensity (MFI) for the evaluation of cell
201 surface markers expression analysis by immunofluorescence using FlowJo software.
202 Data are presented as the mean ± SEM (four mice/group/experiment). **(B)** To analyze
203 antigen phagocytosis, each CLEC10A cDC2 subset sorted from the lungs of ovalbumin
204 (OVA)-primed mice was incubated with 1μg/mL OVA antigen labeled Alexa Fluor 647
205 for 2 hours. **(C)** In addition, the labeled OVA was administered intranasally at the last
206 sensitization to OVA-sensitized mice and cDC2 subsets from the mediastinal lymph
207 nodes and lungs were collected and analyzed. Representative OVA-Alexa Flour 647
208 uptake positive cells gating of CLEC10A^{+} cDC2 (left) and CLEC10A^{-} cDC2 (right)
209 after incubation *in vitro* and sensitization *in vivo*. Numbers indicate the percentage of
210 gated cells in the panel. Graphs showing the percentage of OVA-Alexa Flour 647
211 uptake positive cells on each cDC2 subset. Data are presented as the mean ± SEM (six
212 mice/group/experiment). **(D-F)** To analyze CD4^{+} T cell proliferation and GATA3

213 expression, naïve $CD4^+$ T cells from OVA-specific T-cell receptor transgenic (OT-II)
214 mice were co-cultured with $CLEC10A^+$ and $CLEC10A^-$ cDC2 from the lungs of OVA-
215 primed mice in the presence of 1 μg/mL of OVA for 72 hours. The control group was
216 cultured without cDC2 subsets. **(D)** Representative proliferation cells gating of OT-II
217 $CD4^+$ T cells labeled with CellTrace Far Red, and **(E)** $GATA3^+$ cells gating of OT-II
218 $CD4^+$ T cells after co-culture. Numbers indicate the percentage of gated proliferation
219 cells and $GATA3^+$ cells on OT-II $CD4^+$ T cells in the panel. Percentage graph of
220 proliferation cells and $GATA3^+$ cells on OT-II $CD4^+$ T cells. Data are presented as the
221 mean ± SEM of six independent experiments (four OVA-primed mice and one OT-II
222 mouse/experiment). **(F)** The cytokine levels in the supernatants co-cultured with two
223 cDC2 subsets and OT-II $CD4^+$ T cells were measured by cytometric bead arrays. Data
224 are presented as the mean ± SEM of five independent experiments. **(G)** Cytokine
225 production in response to Toll-like receptor (TLR) ligands. $CLEC10A^+$ and $CLEC10A^-$
226 cDC2 from the lungs of OVA-primed mice were stimulated with 100 ng/mL of
227 PAM_3CSK_4, 1 μg/mL of LPS, or 5 μg/mL of CpG-ODN for 48 hours. The cytokine
228 levels in the supernatants were measured using a cytometric bead array. Data are
229 presented as the mean ± SEM of five independent experiments. ns not significant, *
230 $p<0.05$, ** $p<0.01$, *** $p<0.005$, and **** $p<0.001$.
231

Figure 1

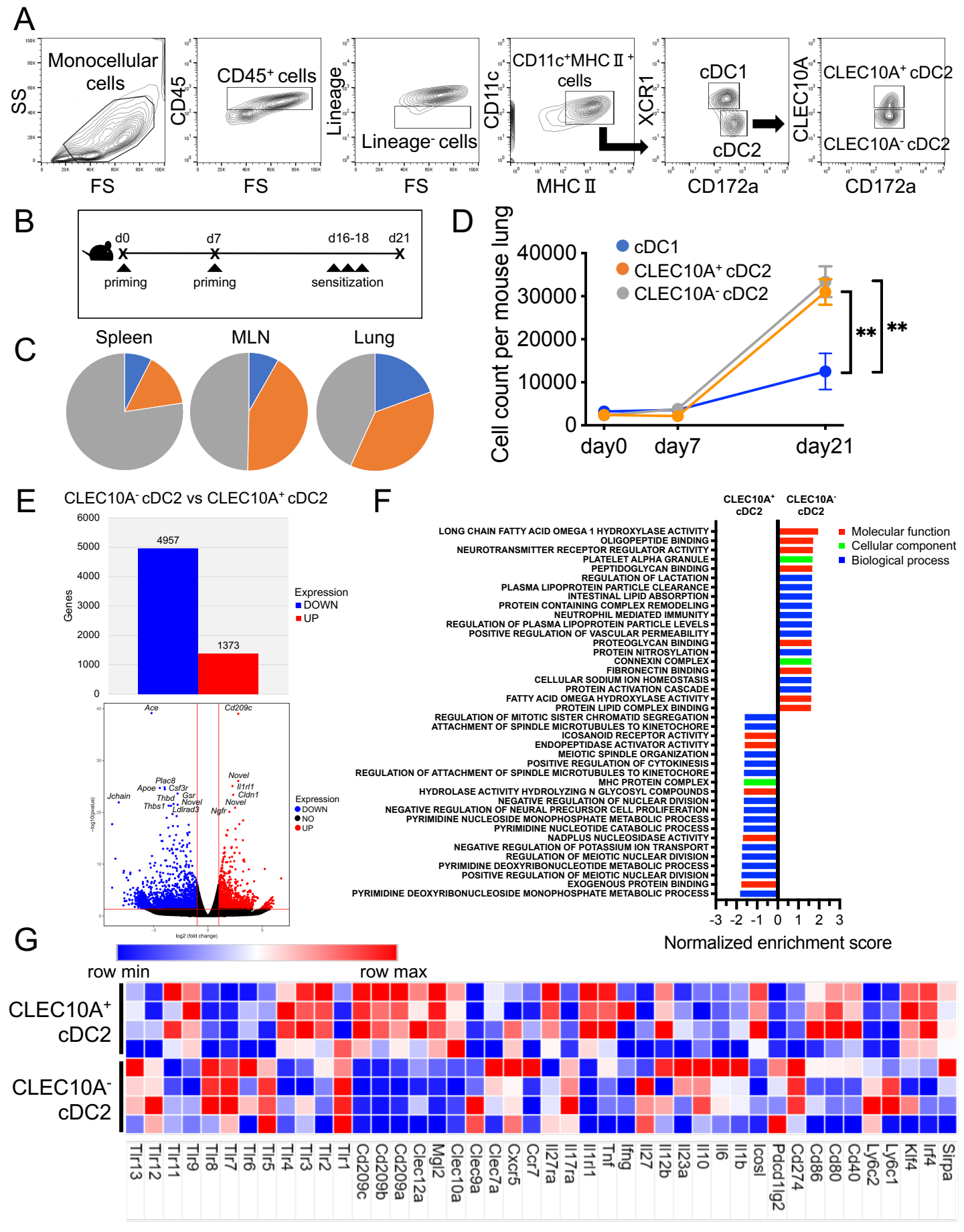
A
Monocellular cells
SS
FS
CD45⁺ cells
CD45
FS
Lineage⁻ cells
Lineage
FS
CD11c⁺MHC II⁺ cells
CD11c
MHC II
cDC1
cDC2
XCR1
CD172a
CLEC10A⁺ cDC2
CLEC10A⁻ cDC2
CLEC10A
CD172a
B
d0
d7
d16-18
d21
priming
priming
sensitization
C
Spleen
MLN
Lung
D
cDC1
CLEC10A⁺ cDC2
CLEC10A⁻ cDC2
Cell count per mouse lung
40000
30000
20000
10000
0
day0
day7
day21
**
**
E
CLEC10A⁻ cDC2 vs CLEC10A⁺ cDC2
Genes
4957
1373
Expression
DOWN
UP
Ace
Cd209c
Plac8
Apoe
Csf3r
Thbd
Gsr
Thbs1
Novel
Ldlrad3
Jchain
Novel
Il1rl1
Cldn1
Novel
Ngfr
Expression
DOWN
NO
UP
log2 (fold change)
F
CLEC10A⁺ cDC2
CLEC10A⁻ cDC2
Molecular function
Cellular component
Biological process
LONG CHAIN FATTY ACID OMEGA 1 HYDROXYLASE ACTIVITY
OLIGOPEPTIDE BINDING
NEUROTRANSMITTER RECEPTOR REGULATOR ACTIVITY
PLATELET ALPHA GRANULE
PEPTIDOGLYCAN BINDING
REGULATION OF LACTATION
PLASMA LIPOPROTEIN PARTICLE CLEARANCE
INTESTINAL LIPID ABSORPTION
PROTEIN CONTAINING COMPLEX REMODELING
NEUTROPHIL MEDIATED IMMUNITY
REGULATION OF PLASMA LIPOPROTEIN PARTICLE LEVELS
POSITIVE REGULATION OF VASCULAR PERMEABILITY
PROTEOGLYCAN BINDING
PROTEIN NITROSYLATION
CONNEXIN COMPLEX
FIBRONECTIN BINDING
CELLULAR SODIUM ION HOMEOSTASIS
PROTEIN ACTIVATION CASCADE
FATTY ACID OMEGA HYDROXYLASE ACTIVITY
PROTEIN LIPID COMPLEX BINDING
REGULATION OF MITOTIC SISTER CHROMATID SEGREGATION
ATTACHMENT OF SPINDLE MICROTUBULES TO KINETOCHORE
ICOSANOID RECEPTOR ACTIVITY
ENDOPEPTIDASE ACTIVATOR ACTIVITY
MEIOTIC SPINDLE ORGANIZATION
POSITIVE REGULATION OF CYTOKINESIS
REGULATION OF ATTACHMENT OF SPINDLE MICROTUBULES TO KINETOCHORE
MHC PROTEIN COMPLEX
HYDROLASE ACTIVITY HYDROLYZING N GLYCOSYL COMPOUNDS
NEGATIVE REGULATION OF NUCLEAR DIVISION
NEGATIVE REGULATION OF NEURAL PRECURSOR CELL PROLIFERATION
PYRIMIDINE NUCLEOSIDE MONOPHOSPHATE METABOLIC PROCESS
PYRIMIDINE NUCLEOTIDE CATABOLIC PROCESS
NADPLUS NUCLEOSIDASE ACTIVITY
NEGATIVE REGULATION OF POTASSIUM ION TRANSPORT
REGULATION OF MEIOTIC NUCLEAR DIVISION
PYRIMIDINE DEOXYRIBONUCLEOTIDE METABOLIC PROCESS
POSITIVE REGULATION OF MEIOTIC NUCLEAR DIVISION
EXOGENOUS PROTEIN BINDING
PYRIMIDINE DEOXYRIBONUCLEOSIDE MONOPHOSPHATE METABOLIC PROCESS
-3 -2 -1 0 1 2 3
Normalized enrichment score
G
row min
row max
CLEC10A⁺ cDC2
CLEC10A⁻ cDC2
Tlr13
Tlr12
Tlr11
Tlr9
Tlr8
Tlr7
Tlr6
Tlr5
Tlr4
Tlr3
Tlr2
Tlr1
Cd209c
Cd209b
Cd209a
Clec12a
Mgl2
Clec10a
Clec9a
Clec7a
Cxcr5
Ccr7
Il27ra
Il17ra
Il1rl1
Tnf
Ifng
Il27
Il12b
Il23a
Il10
Il6
Il1b
Icosl
Pdcd1lg2
Cd274
Cd86
Cd80
Cd40
Ly6c2
Ly6c1
Klf4
Irf4
Sirpa

Figure 2

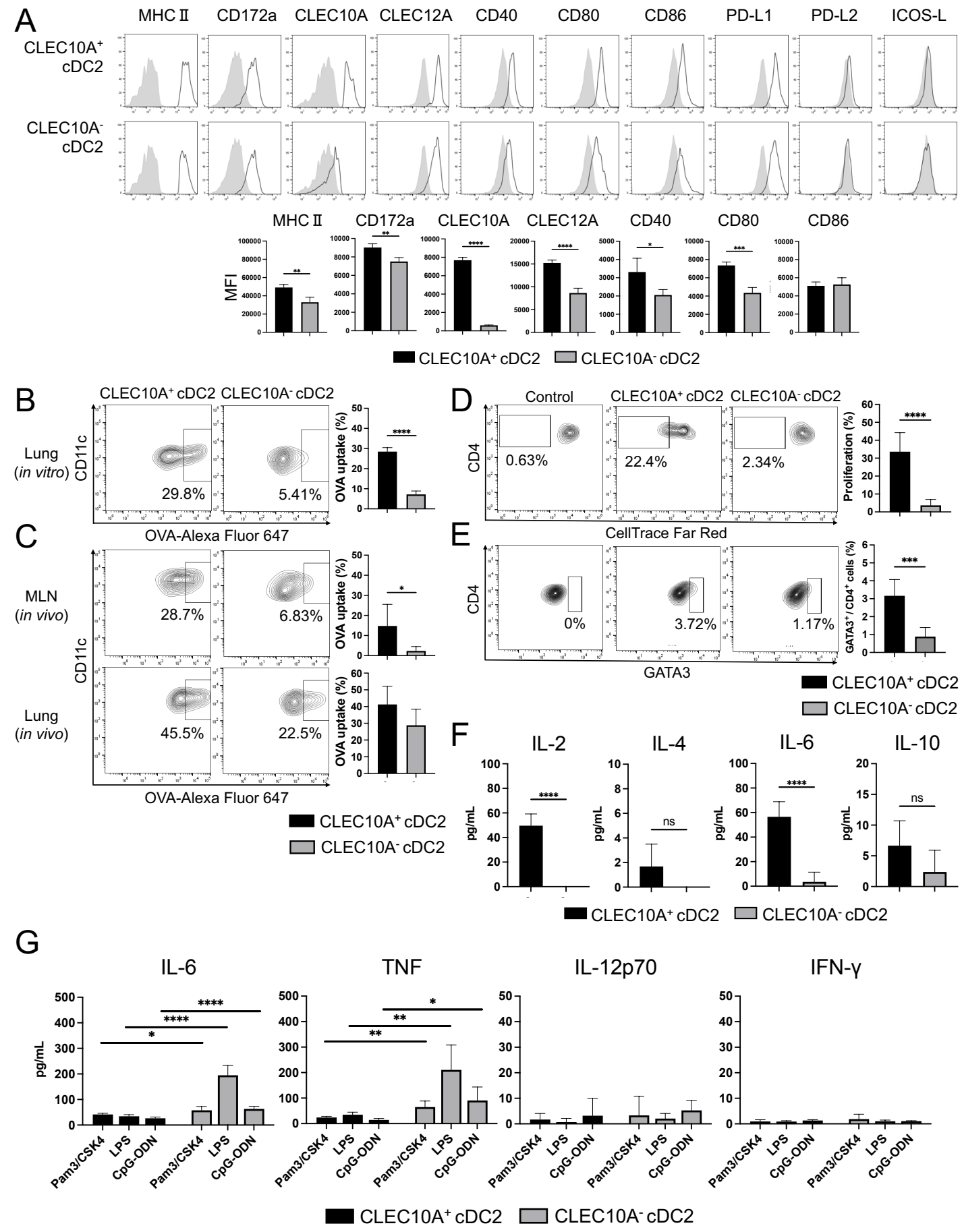
A
MHC Ⅱ
CD172a
CLEC10A
CLEC12A
CD40
CD80
CD86
PD-L1
PD-L2
ICOS-L
CLEC10A+ cDC2
CLEC10A- cDC2
MFI
CLEC10A+ cDC2
CLEC10A- cDC2
B
Lung (in vitro)
CD11c
29.8%
5.41%
OVA-Alexa Fluor 647
OVA uptake (%)
C
MLN (in vivo)
28.7%
6.83%
Lung (in vivo)
45.5%
22.5%
D
Control
0.63%
22.4%
2.34%
CD4
Proliferation (%)
E
CellTrace Far Red
0%
3.72%
1.17%
GATA3
GATA3+ / CD4+ cells (%)
F
IL-2
IL-4
IL-6
IL-10
pg/mL
ns
G
IL-6
TNF
IL-12p70
IFN-γ
Pam3/CSK4
LPS
CpG-ODN

Supplementary Methods

Mice

Experiments were performed using 8–12-week-old male C57BL/6 mice (Nippon-SLC, Shizuoka, Japan) and OVA-specific T-cell receptor (TCR) transgenic mice (OT-II) from the Center for Animal Resources and Development, Kumamoto University, Japan. All experimental protocols were approved by the Animal Care and Use Committee of Hamamatsu University School of Medicine (2020038, 2-13), and all experiments were conducted in accordance with the committee guidelines.

Flow cytometry

Cells were stained with flow cytometry buffer (PBS containing 1% fetal bovine serum and 2 mmol/L EDTA). Cells were stained extracellularly in purified anti-mouse CD16/32 antibody cocktail for 30 min at 4°C. Live/dead cells were differentiated using NIR (Molecular Probes, Eugene, OR, USA), according to the manufacturer's protocol. Flow cytometry was performed using Gallios (Beckman Coulter, Brea, CA, USA) and analyzed using FlowJo 10 (Tree Star, Ashland, OR, USA).

Measurement of cytokine production

The levels of interleukin 2 (IL-2), IL-4, IL-6, IL-10, IL-12p70, interferon-gamma (IFN-γ), and tumor necrosis factor (TNF) in the supernatants were measured using cytometric bead array kits (BD Biosciences, San Jose, CA, USA) according to the manufacturer's instructions.

Preparation of cDC1, CLEC10A$^+$ cDC2, CLEC10A$^-$ cDC2 and naïve CD4$^+$ T cells

Conventional LDC subsets were isolated as previously described,[1] with some modifications. Lungs were excised and enzymatically digested for 40 min at 37°C with 200 IU/mL collagenase type II (Worthington Biochemical, Lakewood, NJ, USA) and 100 IU/mL DNase (Worthington Biochemical). The digested lungs were mechanically dispersed for 30 s using a GentleMACS Dissociator (Miltenyi Biotec, Bergish-Gladbach, Germany). Single-cell suspensions were percolated through a 70 µm cell strainer. The total number of CD11c$^+$ cells was determined by magnetic cell sorting (MACS) (Miltenyi Biotec, Auburn, CA, USA) using anti-CD11c mAb-conjugated magnetic microbeads (Miltenyi Biotec), according to the manufacturer's protocol. CD45$^+$ CD64$^-$ F4/80$^-$ lineage$^-$ MHCII$^+$ CD11c$^+$ XCR1$^+$ CD172a$^-$ LDCs (cDC1), CD45$^+$ CD64$^-$ F4/80$^-$ lineage$^-$ MHCII$^+$ CD11c$^+$ XCR1$^-$ CD172a$^+$ CLEC10A$^+$ LDCs (CLEC10A$^+$ cDC2), and CD45$^+$ CD64$^-$ F4/80$^-$ lineage$^-$ MHCII$^+$ CD11c$^+$ XCR1$^-$ CD172a$^+$ CLEC10A$^-$ LDCs (CLEC10A$^-$ cDC2) were isolated using a MoFlo Astrios EQ (Beckman Coulter). Lineage-negative cells were identified as CD3ε$^-$ CD4$^-$ CD8$^-$ NK1.1$^-$ CD19$^-$ CD45R$^-$ cells. Naïve CD4$^+$ T cells were obtained from the spleens of OT-II mice. The spleens were excised and the cells were suspended by passing through a 70 µm cell strainer. CD4$^+$ Va2$^+$ Vb5$^+$ T cells were isolated using the MoFlo Astrios EQ. The purified conventional LDC subtypes and naïve T cell populations generally contained 95–98% cells. Intracellular staining was performed using APC-labeled anti-T-bet (clone 4B10, Biolegend, San Diego, CA, USA) and True-Nuclear Transcription Factor Buffer Set (Biolegend) according to the manufacturer's instructions.

Ovalbumin priming and sensitization of mice

C57BL/6 mice were inoculated with 50 μg of OVA protein (Sigma-Aldrich, St. Louis, MO, USA) and 2 mg of alum (Thermo Fisher Scientific, Waltham, MA, USA) adjuvant dissolved in 200 μL of PBS via intraperitoneal injection on days 0 and 7. Subsequently, the mice were intranasally sensitized with 50 μg of OVA in 25 μL of PBS on days 16–18. Mice were sacrificed on days 0, 7, and 21 for lung, mediastinal lymph nodes, or spleen collection.

RNA sequencing

Gene expression profiling of conventional LDC subsets was investigated using next-generation sequencing. ISOGEN (Nippon Gene Co., Ltd., Tokyo, Japan) was used for RNA isolation, combined with RNA Clean & Concentrator (Zymo Research, Tustin, CA, USA) and DNase treatment. Total RNA was quantified using a BioAnalyzer RNA Pico Kit (Agilent Technologies Inc., Santa Clara, CA, USA). Approximately 1 ng of total RNA that met the quality guidelines (RIN: ≥ 6.0) was used for cDNA synthesis. cDNA synthesis, followed by library preparation for next-generation sequencing was performed using Smart-Seq Stranded Kit (Takara Bio Inc., Shiga, Japan). The library preparation process involved double-stranded cDNA synthesis using random primers with template-switching technology, which maintained the strand orientation of the original RNA, and cleavage of ribosomal cDNA, preserving both poly-A and non-poly-A mRNA-derived cDNA. A 21-cycle PCR was applied for the addition of Illumina adapters with sample barcodes and library amplification. The resulting cDNA library fragments were examined using Qubit dsDNA Assay (Thermo Fisher Scientific) and TapeStation D1000 ScreenTape (Agilent Technologies Inc., Santa Clara, CA, USA). Individual libraries were then pooled and multiplexed together in equimolar amounts

and sequenced on an Illumina NovaSeq6000 instrument with v1.5 reagents and a 150 bp paired-end configuration. Demultiplexing and FASTQ generation were performed using the bcl2fastq pipeline. Approximately 20 M paired-end reads with a Q30 score > 93 % were obtained for each sample. The FASTQ reads were trimmed to remove the adapter and low-quality sequences. The resulting clean reads were mapped to the reference genome using HISAT2,[2] and gene expression and differential expression analyses between samples were conducted using HT-Seq [3] and DEseq2, [4] respectively. Transcriptome analysis was conducted using GENEWIZ (Azenta Life Sciences, Tokyo, Japan). A heatmap was generated using the Morpheus online tool (https://software.broadinstitute.org/morpheus/). Gene set enrichment analysis (GSEA) [5] was investigated using GSEA software (Broad Institute, Cambridge, MA, USA) (GSEA-MSiDB website, https://www.gsea-msigdb.org/gsea/index.jsp). GSEA was performed using Gene Ontology-based gene set groups (Molecular function, Cellular component, and Biological process). The permutation number was set to 1,000. The criteria used to determine significant enrichment were false discovery rate (FDR) < 0.25 or *p*-value < 0.05. The top 20 of the normalized enrichment score was selected.

Antigen phagocytosis by CLEC10A$^+$ and CLEC10A$^-$ cDC2

Isolated cDC2 subsets from OVA-primed mice (1×10^4 cells/well) were cultured at 37°C with 1μg/mL OVA-Alexa Flour 647 conjugate (Thermo Fisher Scientific) in RPMI-1640 complete medium. After culturing for 2 hours, the cells were harvested and washed twice with fluorescence-activated cell sorting (FACS) buffer. In the mouse model exposed to OVA, Alexa Fluor 647-labeled OVA (Thermo Fisher Scientific) was intranasally administered in the last sensitization to assess the capability of antigen

uptake of cDC2 subsets. OVA antigen phagocytosis of cDC2 subsets was evaluated using FACS.

Priming $CD4^+$ T cells stimulated with $CLEC10A^+$ and $CLEC10A^-$ cDC2

Naïve $CD4^+$ T cells from OT-II mice were incubated with CellTrace™ Far Red Cell Proliferation Kit (Thermo Fisher Scientific). The labeled $CD4^+$ T cells (1×10^5 cells/well) were co-cultured with $CLEC10A^+$ and $CLEC10A^-$ cDC2 from the lungs of OVA-primed mice (1×10^4 cells/well) in the presence of OVA (1 μg/mL) for 72 hours in RPMI-1640 complete medium. The proliferation of $CD4^+$ T cells was assessed using FACS, and the primed $CD4^+$ T cells were collected. Intracellular staining was performed using PE-labeled anti-GATA3 (clone 16E10A23, Biolegend) and True-Nuclear Transcription Factor Buffer Set (Biolegend) according to the manufacturer's instructions. The culture supernatants were collected and stored at –30°C for cytokine measurement.

Treatment of $CLEC10A^+$ and $CLEC10A^-$ cDC2 with Toll-like receptor ligands

Isolated $CLEC10A^+$ and $CLEC10A^-$ cDC2 from the lungs of OVA-primed mice (3×10^4 cells/well) were stimulated with 1 μg/mL of lipopolysaccharide (LPS) (Sigma-Aldrich), 100 ng/mL of PAM_3CSK_4 (Imgenex Corporation, San Diego, CA, USA), or 5 μg/mL of CpG-motif oligodeoxynucleotides (CpG-ODN) (Imgenex), in RPMI complete medium in 96-well round-bottomed plates for 48 hours. The culture supernatants were collected and stored at –30°C for cytokine measurement.

Statistical analysis

The statistical analysis was performed using GraphPad Prism 9.4.1 (GraphPad Software, San Diego, CA, USA). Data were analyzed using the independent samples t-test for comparisons between two groups, and Tukey's test was used for multiple group comparisons. Data are expressed as the mean ± SEM. Statistical significance was set at $p < 0.05$.

References

1. Sakurai S, Furuhashi K, Horiguchi R, Nihashi F, Yasui H, Karayama M, et al. Conventional type 2 lung dendritic cells are potent inducers of follicular helper T cells in the asthmatic lung. *Allergol Int* 2021; **70**: 351-9.
2. Kim D, Langmead B, Salzberg SL. HISAT: a fast spliced aligner with low memory requirements. *Nat Methods* 2015; **12**: 357-60.
3. Mortazavi A, Williams BA, McCue K, Schaeffer L, Wold B. Mapping and quantifying mammalian transcriptomes by RNA-Seq. *Nat Methods* 2008; **5**(7): 621-8. doi: 10.1038/nmeth.1226
4. Love MI, Huber W, Anders S. Moderated estimation of fold change and dispersion for RNA-seq data with DESeq2. *Genome Biol* 2014; **15**(12): 550. doi: 10.1186/s13059-014-0550-8
5. Subramanian A, Tamayo P, Mootha VK, Mukherjee S, Ebert BL, Gillette MA, et al. Gene set enrichment analysis: a knowledge-based approach for interpreting genome-wide expression profiles**.** *Proc Natl Acad Sci U S A*. 2005; **102**: 15545-50. doi: 10.1073/pnas.0506580102.

GeneID	GeneName	Chr	Start	End	Strand	Length	TMP CLEC10A-cDC2-No1	TMP CLEC10A-cDC2-No2	TMP CLEC10A-cDC2-No3	TMP CLEC10A-cDC2-No4	TMP CLEC10A+cDC2-No1	TMP CLEC10A+cDC2-No2	TMP CLEC10A+cDC2-No3	TMP CLEC10A+cDC2-No4	P value
ENSMUSG00000001444	Tbx21	11	97098071	97115331	-	2488	0.815	0.504	0.959	1.13	0.366	0.737	0.307	0.773	NS
ENSMUSG00000020538	Srebf1	11	60199089	60222581	-	6546	2.918	2.654	2.47	2.634	3.058	2.9	2.49	3.525	NS
ENSMUSG00000022463	Srebf2	15	82147181	82205379	+	10231	10.64	8.753	11.649	9.835	14.607	14.055	13.136	12.645	NS
ENSMUSG00000028163	Nfkb1	3	135584655	135691547	-	17011	10.978	8.879	10.491	9.605	10.602	10.262	11.574	9.763	NS
ENSMUSG00000022952	Runx1	16	92601466	92826149	-	24091	3.062	2.968	4.171	3.439	5.28	5.35	4.514	4.086	NS
ENSMUSG00000039153	Runx2	17	44495987	44814797	-	8879	1.298	1.167	2.712	2.235	0.388	0.231	0.502	0.669	1.75E-06
ENSMUSG00000070691	Runx3	4	135120652	135177990	+	12306	6.334	4.986	6.507	4.508	7.184	7.113	6.719	5.401	NS
ENSMUSG00000008193	Spib	7	44525993	44532071	-	4193	0.672	0.982	2.167	1.738	0.465	0.489	0.488	0.532	9.55E-05
ENSMUSG00000004359	Spic	10	88674772	88685015	-	4274	0.637	0.565	0.443	0.203	0.023	0	0.038	0.04	1.45E-08
ENSMUSG00000026565	Pou2f1	1	165865154	166002678	-	16651	0.457	0.481	0.723	0.536	0.884	0.946	0.733	0.6	NS
ENSMUSG00000008496	Pou2f2	7	25087344	25179726	-	9318	3.029	3.436	4.254	2.558	2.201	2.978	2.611	1.828	NS
ENSMUSG00000031162	Gata1	X	7959260	7978071	-	2438	0.065	0.013	0.016	0	0	0	0	0	NS
ENSMUSG00000015053	Gata2	6	88193891	88207032	+	5626	0.197	0.183	0.195	0.191	0.017	0.026	0.171	0.031	0.013694597
ENSMUSG00000015619	Gata3	2	9857078	9890034	-	4318	0.403	0.387	0.123	0.137	0.858	1.141	0.121	0.191	NS
ENSMUSG00000023034	Nr4a1	15	101254269	101274795	+	10615	31.681	23.371	30.655	20.062	30.89	27.879	35.021	18.605	NS
ENSMUSG00000026826	Nr4a2	2	57106830	57124003	-	9337	2.659	1.802	3.175	2.285	3.638	3.611	3.569	2.442	NS
ENSMUSG00000028341	Nr4a3	4	48045153	48086447	+	13135	30.199	20.957	24.877	20.725	31.276	26.726	36.159	22.025	NS
ENSMUSG00000023027	Atf1	15	100227819	100261244	+	3181	3.425	3.146	4.404	2.727	4.118	5.99	4.645	3.713	NS
ENSMUSG00000025958	Creb1	1	64532645	64604548	+	15091	1.305	1.546	2.052	1.897	2.328	2.101	2.6	2.13	NS
ENSMUSG00000032228	Tcf12	9	71842688	72111871	-	16176	1.098	0.71	1.28	0.914	1.465	1.522	1.666	1.31	NS
ENSMUSG00000020167	Tcf3	10	80409514	80433647	-	4483	3.123	2.634	3.513	3.684	4.321	4.322	4.084	4.442	NS
ENSMUSG00000053477	Tcf4	18	69343356	69689079	+	27782	0.613	0.615	1.507	1.16	0.826	0.766	1.15	0.791	NS
ENSMUSG00000039164	Naif1	2	32450457	32456953	+	5176	0.563	0.51	0.578	0.536	1.042	0.528	0.737	0.524	NS
ENSMUSG00000021972	Hmbox1	14	64811600	64949871	-	11318	0.979	1.009	1.472	1.585	1.78	1.969	1.65	1.317	NS
ENSMUSG00000039191	Rbpj	5	53466152	53657362	+	41176	3.139	2.587	2.999	2.277	7.289	7.667	7.604	4.768	1.47E-06
ENSMUSG00000042745	Id1	2	152736251	152737410	+	1240	1.456	1.22	1.374	0.532	0.315	0.638	0.777	0.194	0.010646848
ENSMUSG00000020644	Id2	12	25093799	25097140	-	6379	8.654	5.75	8.718	7.577	13.644	11.474	14.956	11.222	NS
ENSMUSG00000007872	Id3	4	136143497	136145755	+	1841	4.783	3.531	4.997	3.449	2.33	2.578	3.533	1.921	NS
ENSMUSG00000056749	Nfil3	13	52967209	52981073	-	2026	19.932	15.993	14.538	10.703	7.379	7.541	9.117	8.185	4.72E-05
ENSMUSG00000047407	Tgif1	17	70844205	70853546	-	6888	6.58	4.62	5.397	3.884	6.497	5.882	6.698	4.217	NS
ENSMUSG00000062175	Tgif2	2	156840007	156855570	+	4531	1.097	0.859	1.262	0.597	1.09	1.301	0.877	1.129	NS
ENSMUSG00000030557	Mef2a	7	67231163	67372858	-	22201	2.622	2.422	3.209	2.093	2.915	2.568	3.18	2.242	NS
ENSMUSG00000005583	Mef2c	13	83504034	83667080	+	15931	1.551	1.565	2.605	1.803	2.038	2.29	2.158	1.552	NS
ENSMUSG00000001419	Mef2d	3	88142372	88172086	+	6217	7.871	6.454	7.91	6.451	4.846	3.857	4.825	4.484	NS
ENSMUSG00000023994	Nfya	17	48386885	48409906	-	8522	4.17	3.005	4.123	3.159	6.205	5.1	5.452	4.13	NS
ENSMUSG00000024431	Nr3c1	18	39410545	39519421	-	8029	2.962	3.438	4.753	3.487	4.631	4.952	4.896	3.519	NS
ENSMUSG00000003154	Foxj2	6	122819914	122845366	+	5879	2.424	2.353	3.51	2.774	4.749	5.43	5.02	4.742	NS
ENSMUSG00000032998	Foxj3	4	119537004	119629119	+	10973	0.976	0.897	1.266	0.901	1.392	1.625	1.394	1.233	NS
ENSMUSG00000056493	Foxk1	5	142401497	142462011	+	7792	3.634	2.961	4.353	3.709	4.117	3.308	3.025	2.926	NS
ENSMUSG00000039275	Foxk2	11	121259990	121309896	+	6951	2.383	1.944	2.288	2.795	3.876	3.672	3.414	3.132	NS
ENSMUSG00000020275	Rel	11	23736847	23770970	-	15304	13.51	12.346	15.466	11.438	16.524	17.307	20.03	11.635	NS
ENSMUSG00000024927	Rela	19	5637483	5648130	+	3074	18.845	14.152	16.897	15.068	15.806	15.063	17.804	13.526	NS
ENSMUSG00000026815	Gfi1b	2	28609450	28621982	-	1830	0.26	0.527	0.145	0.379	0.142	0.295	0.219	0.019	NS
ENSMUSG00000003847	Nfat5	8	107293470	107379517	+	21595	1.55	1.42	2.083	1.605	1.666	1.705	2.081	1.652	NS
ENSMUSG00000034266	Batf	12	85686669	85709087	+	6617	1.575	1.293	1.299	1.494	1.37	1.657	1.711	1.313	NS
ENSMUSG00000026630	Batf3	1	191097847	191108945	+	2948	3.019	1.986	3.313	2.154	3.947	4.341	2.806	3.75	NS
ENSMUSG00000044167	Foxo1	3	52268336	52353221	+	8899	1.157	1.327	1.944	1.528	2.491	2.189	2.265	1.624	NS
ENSMUSG00000048756	Foxo3	10	42181841	42276755	-	9868	3.704	3.091	3.319	2.848	3.877	4.015	3.084	3.337	NS
ENSMUSG00000042903	Foxo4	X	101254528	101260873	+	3853	1.274	0.743	1.091	0.54	1.012	0.877	1.126	0.909	NS
ENSMUSG00000021366	Hivep1	13	42052021	42192537	+	15072	5.237	4.172	5.702	4.07	5.563	5.25	6.12	4.132	NS
ENSMUSG00000015501	Hivep2	10	13966075	14151374	+	25206	2.827	2.747	3.396	3.076	4.352	5.189	4.91	4.19	NS
ENSMUSG00000028634	Hivep3	4	119733784	120138045	+	24890	1.01	0.932	0.945	0.795	1.235	1.118	1.276	0.949	NS
ENSMUSG00000055435	Maf	8	115682942	115707794	-	8241	1.034	0.953	0.864	0.581	0.213	0.462	0.161	0.142	2.05E-05
ENSMUSG00000074622	Mafb	2	160363703	160367065	-	3363	11.782	10.649	8.24	6.531	4.919	6.339	4	2.532	0.0002306
ENSMUSG00000025612	Bach1	16	87698945	87733346	+	6334	11.151	9.611	11.464	7.077	10.57	8.78	10.378	7.442	NS
ENSMUSG00000040270	Bach2	4	32238804	32586108	+	14066	1.115	0.899	1.443	1.354	1.243	1.14	1.679	1.255	NS
ENSMUSG00000026628	Atf3	1	191170296	191218039	-	27109	10.024	9.272	13.685	8.118	24.962	24.266	22.657	14.686	NS
ENSMUSG00000034271	Jdp2	12	85599027	85639878	+	13489	6.138	4.06	5.195	4.404	4.696	4.856	7.133	4.342	NS
ENSMUSG00000000861	Bcl11a	11	24078056	24174123	+	14265	0.881	0.947	1.948	1.914	1.768	1.633	1.419	2.108	NS
ENSMUSG00000004040	Stat3	11	100885098	100939540	-	9534	12.983	10.422	11.901	8.971	8.083	7.726	8.954	8.502	NS
ENSMUSG00000070031	Sp140	1	85600378	85645037	+	5619	5.642	4.409	4.945	4.625	4.274	4.184	4.131	3.666	NS
ENSMUSG00000005698	Ctcf	8	105636568	105682922	+	5492	3.068	3.164	4.37	4.005	4.776	5.701	4.599	4.501	NS
ENSMUSG00000017801	Mlx	11	101087277	101092207	+	1999	0.016	0	0.019	0	0	0.09	0	0	NS
ENSMUSG00000038648	Creb3l2	6	37327255	37442146	-	7326	1.098	0.703	1.204	0.985	1.318	1.099	0.948	0.9	NS
ENSMUSG00000005897	Nr2c1	10	94148023	94197211	+	4837	0.367	0.293	0.391	0.545	0.699	1.026	0.623	0.575	NS
ENSMUSG00000005893	Nr2c2	6	92091390	92174294	+	15310	1.082	1.16	1.921	1.289	1.373	1.538	1.443	1.446	NS
ENSMUSG00000075028	Prdm11	2	92972018	93046167	-	11384	0.415	0.153	0.279	0.299	0.3	0.174	0.325	0.401	NS
ENSMUSG00000025225	Nfkb2	19	46304320	46312385	+	5318	19.07	15.52	16.238	14.386	16.513	15.467	17.638	15.185	NS
ENSMUSG00000032238	Rora	9	68653786	69388246	+	13554	0.395	0.351	0.528	0.253	0.374	0.504	0.19	0.119	NS
ENSMUSG00000036192	Rorb	19	18930605	19111196	-	11076	0.003	0	0.014	0.034	0	0	0	0.019	NS
ENSMUSG00000028150	Rorc	3	94372794	94398276	+	3559	0.258	0.045	0.128	0.088	0.137	0.01	0.011	0.029	NS
ENSMUSG00000032481	Smarcc1	9	110117708	110240178	+	7911	3.607	2.908	3.757	3.118	3.989	3.585	3.847	3.35	NS
ENSMUSG00000025369	Smarcc2	10	128459248	128490482	+	5902	8.511	8.445	9.494	8.665	12.01	10.476	12.682	10.599	NS
ENSMUSG00000028639	Ybx1	4	119277981	119294604	-	2531	78.499	58.696	73.489	65.279	101.111	102.094	92.541	80.958	NS
ENSMUSG00000029475	Kdm2b	5	122870665	122989823	-	11612	2.376	1.912	2.488	2.238	3.809	2.823	3.5	3.167	NS
ENSMUSG00000014767	Tbp	17	15499888	15528379	+	14143	0.45	0.425	0.618	0.393	0.545	0.544	0.491	0.505	NS
ENSMUSG00000018899	Irf1	11	53770014	53778374	+	4341	10.55	8.109	10.117	8.073	11.066	10.169	12.164	7.893	NS
ENSMUSG00000015522	Arnt	3	95434388	95497240	+	8202	2.479	1.985	2.589	1.891	2.853	2.323	2.624	2.131	NS
ENSMUSG00000055116	Arntl	7	113207465	113314126	+	8528	0.475	0.555	0.697	0.468	0.8	0.658	0.457	0.358	NS
ENSMUSG00000028565	Nfia	4	97772734	98118874	+	11341	0.441	0.204	0.341	0.263	0.37	0.317	0.234	0.239	NS
ENSMUSG00000055053	Nfic	10	81396186	81455635	-	7410	2.616	2.119	2.498	1.934	2.649	2.46	2.487	2.673	NS
ENSMUSG00000001911	Nfix	8	84699876	84800344	-	7900	2.634	1.975	2.19	1.585	2.806	2.548	2.536	2.164	NS
ENSMUSG00000017861	Mybl2	2	163054687	163084688	+	7210	0.101	0.317	0.336	0.106	0.6	0.529	0.39	0.429	NS
ENSMUSG00000026222	Sp100	1	85649988	85709998	+	7584	5.007	3.691	5.197	5.339	4.183	4.868	3.426	3.834	NS
ENSMUSG00000056216	Cebpg	7	35046422	35056573	-	5621	2.479	2.061	2.916	1.913	3.203	3.191	3.1	2.975	NS
ENSMUSG00000034957	Cebpa	7	35119293	35121928	+	2636	14.43	10.559	12.079	10.754	19.284	16.324	16.482	17.87	NS
ENSMUSG00000056501	Cebpb	2	167688915	167690418	+	1504	146.295	125.968	107.812	75.043	29.735	27.966	26.859	23.901	2.64E-15
ENSMUSG00000071637	Cebpd	16	15887286	15891031	+	3746	3.509	3.204	4.012	3.862	4.668	4.75	4.416	5.215	NS